Kirkuk Journal of Science Vol. 19, Iss. 1, p 43-50, 2024. doi:10.32894/kujss.2024.146573.1136

Ground State Properties of Even-Even $^{30-92}$Ca Isotopes Using HFB Theory.

Pshkow F. Mahmood *

Kirkuk Education Directory, Ministry of Education, Kirkuk, Iraq.

***Corresponding author** : : pshkow.f$_{m}$*ahmood@yahoo.com.*

Article Information

Article Type:
Research Article

Keywords:
Nuclear Structure; Ground-state properties; Skyrme-Hartree-Fock-Bogoliubov method; Average binding energy; Quadrupole deformation parameter; Two-nucleon separation energy.

History:
Received: 6 February 2023.
Revised: 10 March 2024.
Accepted: 12 March 2024.
Published Online: 25 March 2024.
Published: 30 March 2024.

Citation: Pshkow F. Mahmood, Ground State Properties of Even-Even $^{30-92}$Ca Isotopes Using HFB Theory, Kirkuk Journal of Science, 19(1), 43-50, 2024, https://doi.org/10.32894/kujss.2024.146573.1136

Abstract

Ground State (GS) Properties of Even-Even $^{30-92}_{20}$Ca isotopes have been studied in frame of Skyrme Hartree-Fock-Bogoliubov using computer program HFBTHO V3.00 with three types of Skyrme interactions (HFB9, SLY4 and SLY5). The calculated nuclear properties including (average binding energy ($^{BE}/_{A}$), two nucleon separation energy (S_{2N}), two neutron shell gap (δ_{2N}), quadrupole deformation parameter (β_2), charge radii (R_{ch}), neutron and proton radii (R_N, R_P) and skin thickness) were compared with the available experimental data and with the results of Finite Range Droplet Macroscopic method (FRDM) and Relativistic Mean Field (RMF) theory. According to Binding energy ($^{BE}/_{A}$), it turns out that it increases directly with increase directly with the increases in neutron number until arrive its Max. value at the region between (N=20-30) which is due to the effect of the two magic numbers (N=20,28), after this region ($^{BE}/_{A}$) start to decrease progressively.

1. Introduction:

Despite passing more than a century on the discovery of nuclear physics, scientists are still seeking to reach a universal theory that be able to clarify the general description about nuclear structure properties and the shape of nucleus of all well-known nuclei with high accuracy [1, 2, 3]. Therefore, the essential objective of theoretical researches in this field is to understand the reaction properties, shape, size and structure of each of the nuclei in the periodic table [4, 5, 6].

The essential problems that prevent a microscopic elucidation of nuclei are their complex structure and the nature of nuclear force [7, 8, 9, 10], and to get rid of these two problems many theories and models have been built. Starting from direct solution and speculative models before moving on to more complex ones. For nuclei with small proton number such as ($^{4}_{2}$He, $^{7}_{3}$Li,...), it is possible to use direct solution beginning with a minimal degree of freedom for nucleons [11, 12]. However, due to their extremely high error ratio, these descriptions cannot be compared with the experimental data [13, 14].

Otherwise, to describe light and medium nuclei (nuclei with mass number A<60) a significant progress has been made utilizing the quantum chromodynamics (QCD) [15] and constrained with the Exp. data. This mechanism is known as the ab-initio model and is dependent on nucleon-nucleon interactions [16].

Also, no-core Shell Model [17] can be used for light nuclei, whilst, for nuclei which have mass number up to A = 60, coupled cluster model or self-consistent green function model can be used. for more details, see Refs. [18, 19, 20, 21]. Nonetheless, the nuclear models are divided into three kinds.

1. macroscopic approach such as Bethe Weizcker mass formula based on the liquid drop model [22].

2. macroscopic-microscopic model such as Finite-Range-Droplet-Macroscopic method (FRDM) [23].

3. microscopic models such as the conventional Hartree-Fock (HF) method [24].

The typical and most popular microscopic model that utilized in the nuclear research is the Hartree-Fock (HF) particularly Hartree-Fock-Bogoliubov model, it uses Bardeen Cooper Schrieffer (BCS) pairing theory to generalize HF theory [25].

HF+BCS gives a perfect depiction of the structure of nucleus and GS properties for nuclei close to the line of β-stability. While, for nuclei far away from β-stability line the effectiveness of the pairing correlations are raises progressively, Consequently, to deal with nuclei nearby proton and neutron drip lines, this model is no longer suitable.

Wherefore, Hartree-Fock-Bogoliubov was developed to take into account both of mean-field correlations and pairing correlations self-consistently [26, 27].

Calcium ($^{30-92}_{20}Ca$) with magic proton number (Z=20) and three magic neutron number (N=20,28 and 50) has received great attention in nuclear physics research, in the study of astrophysics the microscopic structure of Ca nucleus has a particular interest [28], nuclei with N $\approx$ 28 play an essential role in the nucleosynthesis of Ca isotopes [29].

After iron and aluminum, Ca is the third most prevalent metal and the fifth most plentiful element in the crust of the Earth. The Ca nucleus have five stable isotopes ($^{40}_{20}Ca$, $^{42}_{20}Ca$, $^{43}_{20}Ca$, $^{44}_{20}Ca$ and $^{46}_{20}Ca$) and A semi-stable isotope ($^{48}_{20}Ca$) so Calcium is the first light element with six naturally occurring isotopes.

In this manuscript, average binding energy, two nucleon separation energy, two neutron shell gap and proton, neutron and charge radii for even-even Ca isotopes were studied. Computer program HFBTHO version 3.00 [30] was used in the present paper with three kinds of Skyrme functional (HFB9 [31], SLY4 [32, 33] and SLY5 [32]). This manuscript is regulated as follows: Hartree-Fock-Bogoliubov model are provided in section 2, In section 3, results and discussions are provided. lastly, in section 4 we present the conclusion of the study.

2. Hartree Fock Bogoliubov Approach:

A Hamiltonian of a many fermion systems can be expressed using set of annihilation (c) operator, and creation (c†) operator [34],

$$H = \sum_{\ell_a \ell_b} t_{\ell_a \ell_b} c_a^\dagger c_{\ell b} + \frac{1}{4} \sum_{\ell_a \ell_b \ell_c \ell_d} \bar{v}_{\ell_a \ell_b \ell_c \ell_d} c_a^\dagger c_b^\dagger c_{\ell_d} c_{\ell_c} \quad (1)$$

where the kinetic energy is represented by the first term, and $\bar{v}_{\ell_a \ell_b \ell_c \ell_d} = v_{\ell_a \ell_b \ell_c \ell_d} - v_{\ell_a \ell_b \ell_d \ell_c}$ are anti-symmetrized matrix-element of two-body interaction. So, the GS wave-function of Hartree Fock Bogoliubov model can be clarified by quasi-particle operators ($\beta_\alpha^\dagger$ and β_α) with a liner transformation of Bogoliubov [35],

$$\beta_\alpha^\dagger = \sum_\ell U_{\ell_a} c_\ell^\dagger + V_{\ell_a} c_\ell \qquad \beta_\alpha = \sum_\ell U_{\ell_a}^* c_\ell + V_{\ell_a}^* c_\ell^\dagger \quad (2)$$

U and V matrices should be satisfying the relations,

$$\begin{aligned} UV^\dagger + V^* U^T = 0,\ U^\dagger U + V^\dagger V = 1, \\ U^T V + V^T U = 0,\ UU^\dagger + V^* V^T = 1 \end{aligned} \quad (3)$$

The single body density matrix in terms of the k and normal ρ is defines as

$$\rho_{kk'} = \langle \Phi | c_k^\dagger, c_k | \Phi \rangle, \qquad k_{kk'} = \langle \Phi | c_k, c_k | \Phi \rangle \quad (4)$$

The energy functional of equation 1 is showed as,

$$E[\rho, k] = \frac{\langle \Phi | H | \Phi \rangle}{\langle \Phi | \Phi \rangle} = Tr\left[t + \frac{1}{2}\Gamma\right]\rho - \frac{1}{2} Tr[\Delta k^*] \quad (5)$$

Where

$$\Gamma_{\ell_a \ell_c} = \sum_{\ell_b \ell_d} \bar{v}_{\ell_a \ell_b \ell_c \ell_d} \rho_{\ell_d \ell_{b'}} \qquad \Delta_{\ell_a \ell_b} = \sum_{\ell_b \ell_d} \bar{v}_{\ell_a \ell_b \ell_c \ell_d} k_{\ell_c \ell_d} \quad (6)$$

The matrix form of the Hartree Fock Bogoliubov equations is provided by,

$$\begin{pmatrix} t+\Gamma-\lambda & \Delta \\ -\Delta^* & -(t+\Gamma-\lambda)^* \end{pmatrix} \begin{pmatrix} U_a \\ V^a \end{pmatrix} = E_a \begin{pmatrix} U_a \\ V^a \end{pmatrix} \quad (7)$$

where (Δ) represent pairing potential, and the fermi energy of the system is represented by Lagrange multiplier (λ) , for more details see ref. [35, 36, 37, 38, 39].

3. Results and Discussions:

In this section, the obtained result in this study was presented and discussed, mostly for (average binding energy ($^{BE}/_{A}$), two nucleon separation energy (S_{2N}), two neutron shell gap (δ_{2N}), quadrupole deformation parameter (β_2), charge radii (R_{ch}), neutron and proton radii (R_N, R_P) and skin thickness). The calculations were done in frame of the HFB approach with three types of Skyrme interactions (HFB9, SLY4 and SLY5).

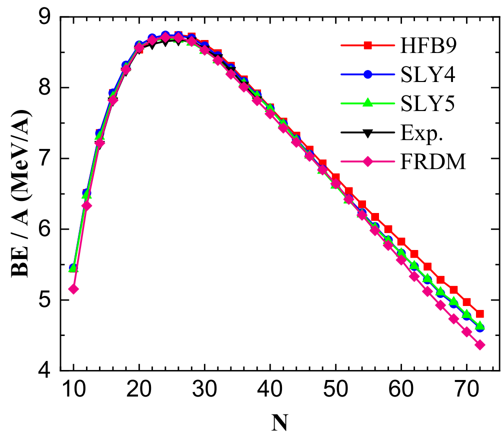

Figure 1. Average binding energy as a function of N.

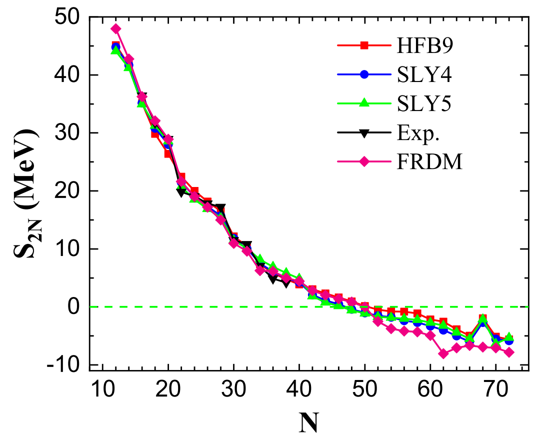

Figure 2. S_{2N} as a function of N.

3.1 Average Binding Energy ($^{BE}/_{A}$):

Average Binding energy ($^{BE}/_{A}$) is one of the most important quantities in the study of nuclear structure, it has a direct relationship with the stability of nucleus [40]. In Figure 1, BE/A as a function of N are presented for Ca isotopes. Our calculated results by HFB9, SLY4 and SLY5 interactions are compared with the results from FRDM 2012 [23] and with the available experimental data [41]. A clear coordination can be seen between our calculated data and the available experimental data and also with FRDM [23] model data.

As shown in Figure 1 $^{BE}/_{A}$ start with about 5.44 MeV and increases gradually with neutron number (N) rise, it reaches its Max. value in the region between (N=20-30) which is due to the effect of doubly magic number (N=20,28 and Z=20) after this region $^{BE}/_{A}$ start to decrease progressively.

3.2 Two Nucleon Separation Energy (S_{2N}):

The fundamental quantity in the studying of nuclear physics is S_{2N}. The calculate values of S_{2N} of $^{30-92}_{20}Ca$ isotopes are shown in Figure 2 using three kinds of Skyrme interactions (HFB9, SLY4 and SLY5), in comparison with the data of FRDM 2012 [23], and with the available experimental data [41].

The S_{2N} value starts with a high value, which is about 45 MeV and then gradually decreases with increasing in N, a sharp decrease happen at magic number (N=20,28) because of the effect of closed shell, whereas, when N=50 the effect of the magic number has no appear because approaching the neutron drip line; isotopes were located nearby the drip line have lower S_{2N} values than isotopes located nearby valley of stability.

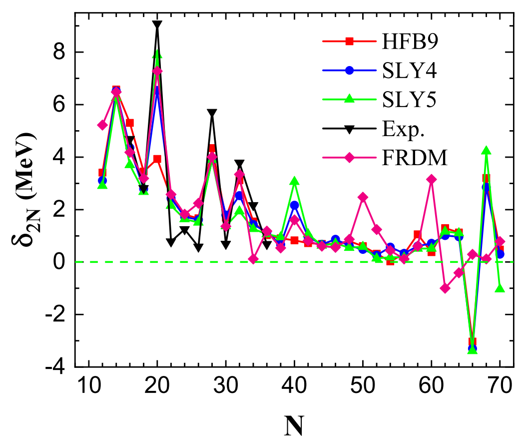

Figure 3. δ_{2N} as a function of N.

3.3 Two Neutron Shell Gap (δ_{2N}):

δ_{2N} has important rule in the study of nuclei far from the valley of stability, the disappearance of the shell effect is defined as the two-neutron shell gap. Eq. 8 clarify δ_{2N} value [6].

$$\delta_{2N}(N,Z) = S_{2N}(N,Z) - S_{2N}(N+2,Z) \tag{8}$$

δ_{2N} values for isotopic chains of Ca nucleus are presented in Figure 3, using three types of Skyrme interactions (HFB9, SLY4 and SLY5), to confirm the validity of the results, they were compared with FRDM [23] data, and with the available experimental data [41]. When N=12, $\delta_{2N} \approx 3.2$ MeV while, when N=14, $\delta_{2N} \approx 6.55$ MeV it has become almost twice what it was since there are twice number of neutrons in $1d_{5/2}$ shell, secondary shell filled; the second and third picks appear

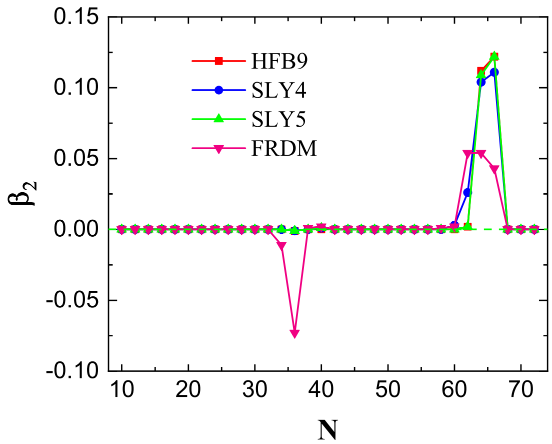

Figure 4. β_2 as a function of N.

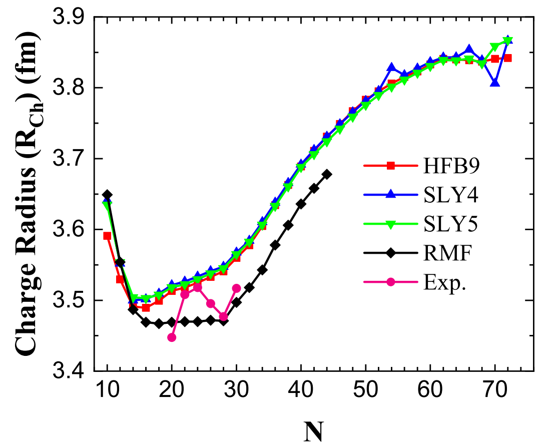

Figure 5. R_c as a function of N.

when N=20,28 N=40 when 2p$_{1/2}$ shell filled, and the last pick appear when N=68 due to 2d$_{3/2}$ shell filled.

3.4 Quadrupole Deformation Parameter (β_2):

β_2 provides us a clear visualization of the shape of isotopes. The calculated β_2 values are presented in Figure 4 as a function of a N for $^{30-92}_{20}Ca$ isotopes using three Skyrme functional (HFB9, SLY4 and SLY5). The calculate result are compared with FRDM 2012 [23]. There is a good agreement among all function. β_2 is defined as in Eq. 9 [35].

$$\beta_2 = \sqrt{\frac{\Pi}{5}} \frac{\langle \hat{Q} \rangle}{\langle r^2 \rangle} \tag{9}$$

Most of Ca isotopes appear with spherical shape due to a magic proton number and three magic neutron numbers, except some isotopes in the region (N=64 and 66) which appear with prolate shape.

3.5 Charge Radius (R_c):

Our HFB calculations of R_c by three Skyrme functional (HFB9, SLY4 and SLY5) are presented in Figure 5 as a function of N, in comparison with the RMF theory data [42] and also with the available experimental data [43]. A clear coordination between the calculated results and the experimental results has been achieved as well as with RMF theory data. R_c is defined in Eq. (10) [30]

$$R_{ch} = \sqrt{\langle r_p \rangle^2 + \langle R_p \rangle^2 + \frac{N}{Z}\langle R_n \rangle^2 + \frac{3}{4M_p^2}} \tag{10}$$

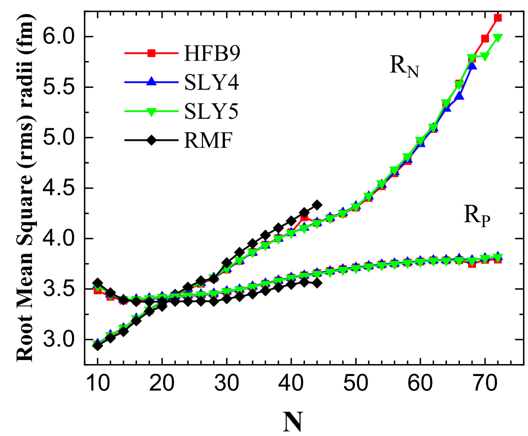

Figure 6. Root Mean Square (rms) radii as a function of N.

The charge radius in primary isotopes decreases because the effect of the closed shell at magic number. After passing magic number it increases with increasing in N.

3.6 Proton and Neutron Root Mean Square (rms) radii:

In Figure 6 we present proton and neutron rms radii together as a function of N in comparison with the values of relativistic mean field (RMF) theory [42]. As shown in Figure 6, proton radius increases slightly as the number of neutrons increases; while, neutron radius increases clearly with the increase in neutron number.

3.7 Skin-Thickness $\Delta r_{N,P}$:

The difference between the neutrons rms radii and protons rms radii is defined as Skin-Thickness $\Delta r_{N,P}$ $\Delta r_{N,P}$ = R_N-R_P). Figure 7 presents $\Delta r_{N,P}$ for Ca isotopic chains calculated by

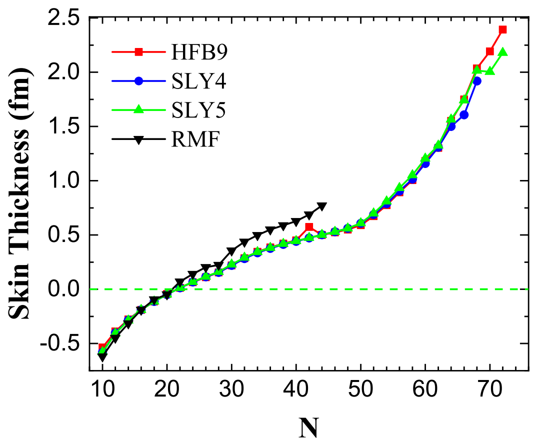

Figure 7. Skin-thickness $\Delta r_{N,P}$ as a function of N.

three types of Skyrme functional (HFB9, SLY4 and SLY5) in comparison with the values of relativistic mean field (RMF) [42] theory. From Figure 7 it can be seen that the additional neutrons lead to the $\Delta r_{N,P}$. Good agreement can be seen between HFB9, SLY4 and SLY5 (this work) results and RMF theory. When neutron number increase $\Delta r_{N,P}$ grows progressively, for Ca isotopes it reaches its maximum value near neutron drip-line.

4. Conclusion:

In the current study, the ground state (GS) properties, including average binding energy, two nucleon separation energy, two neutron shell gap, quadrupole deformation parameter, charge radii, neutron and proton radii and skin thickness) of Ca nuclei have been studied.

Regarding binding energy, $^{BE}/_{A}$ increases directly in Ca isotopes with the increase in neutron number until arrive its maximum value at the region between (N=20-30) which is due to the effect of two magic number (N=20,28), beyond this region $^{BE}/_{A}$ start to decrease progressively.

While, regarding to two neutron separation energy, the S_{2N} starts with a high value which is about 45 MeV and then progressively decreases with increasing in N, the effect of closed-shell appears at N = 20, 28. However, N = 50, this effect has no appear because of approaching the neutron drip line. Concerning two neutron shell gap, δ_{2N} appears picks when N = 14, 20, 28, 32, 40 and 68 due to subshells ($1d_{5/2}$, $2s_{1/2}$, $1d_{5/2}$, $1f_{7/2}$, $2p_{3/2}$, $2p_{1/2}$ and $2d_{3/2}$) that are filled.

As for quadrupole deformation parameter due to magic proton number and three magic neutron numbers most of Ca isotopes appear with spherical shape. Whilst, according to nuclear radii (charge, neutron and proton radii) neutron rms radii increase clearly with the increase in neutron number; while, proton rms increases slightly as the number of neutrons increases.

Funding: None.

Data Availability Statement: All of the data supporting the findings of the presented study are available from corresponding author on request.

Declarations:

Conflict of interest: The authors declare that they have no conflict of interest.

Ethical approval: The manuscript has not been published or submitted to another journal, nor is it under review.

References

[1] T. D. Morris, J. Simonis, S. R. Stroberg, C. Stumpf, G. Hagen, J. D. Holt, G. R. Jansen, T. Papenbrock, R. Roth, and A. Schwenk. Structure of lightest Tin isotopes. *Physical Review Letters*, 120: 152503, 2018, doi:10.1103/PhysRevLett.120.152503.

[2] V. Som'a, C. Barbieri, T. Duguet, and P. Navrátil. Moving away from singly-magic nuclei with gorkov green's function theory. *The European Physical Journal A*, 57: 135, 2021, doi:10.1140/epja/s10050-021-00437-4.

[3] S. R. Stroberg, J. D. Holt, A. Schwenk, and J. Simonis. Ab initio limits of atomic nuclei. *Physical Review Letters*, 126, 2021, doi:10.1103/PhysRevLett.126.022501.

[4] Ali H. Taqi and Pshkow F. Mahmood. Ground state properties and shape transition of even-even 76Os, 78Pt, 80Hg and 82Pb isotopes in the framework of skyrme hartree-fock-bogoliubov theory. *Arab Journal of Nuclear Sciences and Applications*, 55(1): 34, 2023, doi:10.21608/ajnsa.2021.70418.1461.

[5] Y. El Bassem and M. Oulne. Ground state properties and shape evolution in pt isotopes within the covariant density functional theory. *International Journal of Modern Physics E*, 49(10): 08775, 2019, doi:10.1142/S0218301319500782.

[6] Ali H. Taqi and Pshkow F. Mahmood. Nuclear structure investigation of even-even isotopes from Sn to Pb. *Iranian Journal of Science and Technology, Transection A: Science*, 45(49), 2023, doi:10.1007/s40995-021-01174-5.

[7] Aurel Bulgac and et. al. A minimal nuclear energy density functional. *Physical Review C*, 97(4): 044313, 2018, doi:10.1103/PhysRevC.97.044313.

[8] E. Caurier, G. Mart´ınez-Pinedo, F. Nowacki, A. Poves, and A. P. Zuker. The shell model as a unified view of nuclear structure. *Reviews of Modern Physics*, 77: 427–488, 2005, doi:10.1103/RevModPhys.77.427.

[9] P. Navr´atil, S. Quaglioni, I. Stetcu, and B. R. Barrett. Recent developments in no-core shell-model calculations. *Journal of Physics G*, 36: 083101, 2009, doi:10.1088/0954-3899/36/8/083101.

[10] E. F. Dumitrescu, A. J. McCaskey, G. Hagen, G. R. Jansen, T. D. Morris, T. Papenbrock, R. C. Pooser, D. J. Dean, and P. Lougovski. Cloud quantum computing of an atomic nucleus. *Physical Review Letters*, 120: 210501, 2018, doi:10.1103/PhysRevLett.120.210501.

[11] S. Bacca. Structure models: From shell model to ab initio methods a brief introduction to microscopic theories for exotic nuclei. *The European Physical Journal Plus*, 131, 2016, doi:10.1140/epjp/i2016-16107-6.

[12] Pshkow F. Mahmood. Hartree-fock-bogoliubov calculations of ground-state properties for even-even neutron-rich nuclei. Master's thesis, 2021.

[13] S. R. Beane and et. al. Light nuclei and hypernuclei from quantum chromodynamics in the limit of SU(3) flavor symmetry. *Physical Review D*, 87: 034506, 2013, doi:10.1103/PhysRevD.87.034506.

[14] S. R. Beane and et. al. Magnetic moments of light nuclei from lattice quantum chromodynamics. *Physical Review Letters*, 113: 252001, 1966, doi:10.1103/PhysRevLett.113.252001.

[15] H.-W. Hammer, S. König, and U. van Kolck. Nuclear effective field theory: Status and perspectives. *Reviews of Modern Physics*, 92: 025004, 2020, doi:10.1103/RevModPhys.92.025004.

[16] S. R. Beane and et. al. Ab initio calculation of the np $\rightarrow d\gamma$ radiative capture process. *International Journal of Medical Pharmaceutical Sciences*, 115: 132001, 2015, doi:10.1103/PhysRevLett.115.132001.

[17] P. Navratil and et. al. Recent developments in no-core shell-model calculations. *Journal of Physics G: Nuclear and Particle Physics*, 36: 083101, 2009, doi:10.1088/0954-3899/36/8/083101.

[18] C. Barbieri and M. Hjorth-Jensen. Quasiparticle and quasihole states of nuclei around ^{56}Ni. *Physical Review C*, 79: 064313, 2009, doi:10.1103/PhysRevC.79.064313.

[19] H. Bohr, C. Providencia, and J. da Providencia. Nuclear phenomena derived from quark-gluon strings. *Physical Review C*, 71: 055203, 2005, doi:10.1103/PhysRevC.71.055203.

[20] G. Hagen and et. al. Ab initio coupled-cluster approach to nuclear structure with modern nucleon-nucleon interactions. *Physical Review C*, 82: 034330, 2010, doi:10.1103/PhysRevC.82.034330.

[21] G. Hagen, T. Papenbrock, D. J. Dean, and M. Hjorth-Jensen. Medium-mass nuclei from chiral nucleon-nucleon interactions. *Physical Review Letters*, 101: 092502, 2008, doi:10.1103/PhysRevLett.101.092502.

[22] J. Meng and P. Ring. Giant halo at the neutron drip line. *Physical Review Letters*, 80: 460, 1998, doi:10.1103/PhysRevLett.80.460.

[23] P. Möller, A. J. Sierk, T. Ichikawa, and H. Sagawa. Nuclear ground-state masses and deformations: Frdm. *Atomic Data and Nuclear Data Tables*, 109: 1, 2016, doi:10.1016/j.adt.2015.10.002.

[24] A N Antonov and et. al. Temperature dependence of the symmetry energy and neutron skins in Ni Sn and isotopic chains. *Physical Review C*, 95: 024314, 2017, doi:10.1103/PhysRevC.95.039903.

[25] M. Yamagami, K. Matsuyanagi, and M. Matsuo. Symmetry-unrestricted skyrme–hartree–fock–bogoliubov calculations for exotic shapes in N =Z nuclei from ^{64}Ge to ^{84}Mo. *Nuclear Physics A*, 693: e03038–22, 2001, doi:10.1016/S0375-9474(01)00918-6.

[26] T. R. Werner and et. Al. Shape coexistence around 1624S28: The deformed N=28 region. *Physics Letters B*, 333: 303, 1994, doi:10.1128/spectrum.01544-23.

[27] Ali H. Taqi and Malik A. Hasan. Ground state properties of even-even nuclei from he (Z=2) to Ds (Z=110) in the framework of skyrme hartree-fock-bogoliubov theory. *Arabian Journal of Science and Engineering*, 47: 761, 2022, doi:10.1007/s13369-021-05345-9.

[28] T. R. Werner and et. Al. Ground-state properties of exotic Si, S, Ar and Ca isotopes. *Nuclear Physics A*, 597(3): 327–340, 1996, doi:10.1016/0375-9474(95)00476-9.

[29] O. Sodin and et. Al. Decay properties of exotic n $\simeq$ 28 s and cl nuclei and the $^{48}Ca/^{46}Ca$ abundance ratio. *Physical Review C*, 47: 2941, 1993, doi:10.1103/PhysRevC.47.2941.

[30] R. Navarro Perez and et. Al. Axially deformed solution of the skyrme-hartree-fock-bogolyubov equations using the transformed harmonic oscillator basis (III) hfbtho (v3.00): a new version of the program. *Computer Physics Communications — Journal*, 220: 363, 2017, doi:10.1016/j.cpc.2017.06.022.

[31] M. Kortelainen and et al. Nuclear energy density optimization: Large deformations. *Physical Review C*, 85(2): 024304, 2012, doi:10.1103/PhysRevC.85.024304.

[32] E. Chabanat, P. Bonche, P. Haensel, J. Meyer, and R. Schaeffer. A skyrme parametrization from subnuclear to neutron star densities part II. nuclei far from stabilities. *Nuclear Physics A*, 635(1-2): 231–256, 1998, doi:10.1016/S0375-9474(98)00180-8.

[33] Wafaa A. Mansour and Ali H. Taqi. Isoscalar giant dipole resonance of tin isotopes ^{112,114,116,118,120,122,124}Sn using HF- BCS and QRPA Approximation. *Kirkuk Journal of Science*, 18(4): 42, 2023, doi:10.32894/KUJSS.2023.145104.1126.

[34] M. V. Stoitsov and et. al. Axially deformed solution of the skyrme-hartree–fock–bogoliubov equations using the transformed harmonic oscillator basis (II) HFBTHO v2.00d: A new version of the program. *Computer Physics Communications*, 184: 1592, 2013, doi:10.1016/j.cpc.2013.01.013.

[35] M. V. Stoitsov and et. al. Axially deformed solution of the skyrme-hartree-fock-bogoliubov equations using the transformed harmonic oscillator basis. the program HFBTHO (v1.66p). *Computer Physics Communications*, 167: 43, 2005, doi:10.1016/j.cpc.2005.01.001.

[36] M. Bender, P.-H. Heenen, and P.-G. Reinhard. Self-consistent mean-field models for nuclear structure. *Reviews of Modern Physics*, 75: 121, 2003, doi:10.1103/RevModPhys.75.121.

[37] J. Dobaczewski, H. Flocard, and J. Treiner. Hartree-fock-bogolyubov description of nuclei near the neutron-drip line. *Nuclear Physics A*, 422: 103, 1983, doi:10.1016/0375-9474(84)90433-0.

[38] E. Perlińska and et. al. Local density approximation for proton-neutron pairing correlations: Formalism. *Physical Review C*, 69: 014316, 2004, doi:10.1103/PhysRevC.69.014316.

[39] P. Ring and P. Schuck. *The Nuclear Many-Body Problem*. Springer-Verlag, New York, 1st edition, 1980.

[40] J. S. Lilley. *Nuclear Physics principle and application*. Willey, England, 2001.

[41] M. Wang and et. al. The ame2016 atomic mass evaluation (II). tables, graphs and references. *Physical Review C*, 41: 030003, 2017, doi:10.1088/1674-1137/41/3/030003.

[42] G. A. Lalazissis, S. Raman, and P. Ring. Ground-state properties of even-even nuclei in the relativistic mean-field theory. *Atomic Data and Nuclear Data Tables*, 71: 1–40, 1999.

[43] I. Angeli and K. P. Marinova. Table of experimental nuclear ground state charge radii: An update. *Atomic Data and Nuclear Data Tables*, 99: 69, 2013.

خصائص المستوى الارض لنظائر $^{30-92}Ca$ الزوجيةالزوجية باستخدام نظرية HFB

بشكو فاتح محمود *

مديرية تربية كركوك، وزارة التربية، كركوك، العراق.

* الباحث المسؤول: pshkow.$f_m$ahmood@yahoo.com

الخلاصة

تم الدراسة خصائص المستوى الارضي لنظائر $^{30-92}Ca$ الزوجية – الزوجية في اطار نظرية سكيرمي هارتري فوك بوغرليوبوف ($Hartree-Fock-Bogoliubov\ Skyrme$) باستخدام برنامج حاسوب ($V3.00\ HFBTHO$) مع ثلاثة أنواع من تفاعلات سكيرمي ($SLY5$ ، $SLY4$ ، $HFB9$)، الخواص النووية المحسوبة تضمنت كل من (معدل طاقة الربط النووية، طاقة فصل النيوترونات، فجوة غلاف النيوترونات، التشوه الرباعي، نصف قطر الشحنة، نصف قطر النيوترون والبروتون وسمك القشرة)، تم مقارنة النتائج مع البيانات االعملية المتوفرة ومع نتائج طريقة ($FRDM$) ونظرية المجال النسبي (RMF) من خلال النتائج المحسوبة تبين ان طاقة الربط في نظائر الكالسيوم تزداد مباشرة مع زيادة عدد النيوترونات و تصل إلى أقصى الحد في المنطقة الواقعة بين ($N=20-30$) والتي ترجع إلى تأثير الرقمين السحريين ($N=20,28$) و بعد هذه المنطقة تبدأ طاقة الربط في التناقص تدريجياً.

الكلمات الدالة: التركيب النووي؛ خصاص المستوى الارضي؛ طريقة سكرمي هارتري بوغوليوبوف؛ معدل طاقة الربط؛ معامل التشويه الرباعي؛ طاقة فصل نيكوليونين.

التمويل: لايوجد.

بيان توفر البيانات: جميع البيانات الداعمة لنتائج الدراسة المقدمة يمكن طلبها من المؤلف المسؤول.

اقرارات:

تضارب المصالح: يقر المؤلفون أنه ليس لديهم تضارب في المصالح.

الموافقة الأخلاقية: لم يتم نشر المخطوطة أو تقديمها لمجلة أخرى، كما أنها ليست قيد المراجعة.